

Running α_s from Landau-gauge gluon and ghost correlations

A. Sternbeck^{*}, K. Maltman[†], L. von Smekal and A. G. Williams

*Centre for the Subatomic Structure of Matter (CSSM), Department of Physics,
University of Adelaide, SA 5005, Australia*

E-mail: andre.sternbeck@adelaide.edu.au

E.-M. Ilgenfritz and M. Müller-Preussker

Humboldt-Universität zu Berlin, Institut für Physik, 12489 Berlin, Germany

We estimate the running coupling constant of the strong interactions within the nonperturbative framework of lattice QCD in Landau gauge. Our calculation is based on the ghost-gluon vertex which in the particular case of Landau gauge allows for a definition of α_s in a MOM scheme solely in terms of the gluon and ghost dressing functions. As a first step we investigate the zero and two-flavour case and report here on preliminary results.

The XXV International Symposium on Lattice Field Theory

July 30 – August 4, 2007

Regensburg, Germany

^{*}Speaker.

[†]And Department of Mathematics and Statistics, York Univ., Toronto, ON, M3J 1P3, Canada.

1. Introduction

The renormalised QCD coupling $\alpha_s = g^2/(4\pi)$ is one of the fundamental parameters of the Standard Model of particle physics and can not only be determined from high-energy experiments but also estimated directly in lattice QCD simulations (see, e.g., [1] for a recent review).

The actual values of α_s depend on both the renormalisation scheme (including the number of active flavours) and the scale considered. Given a renormalisation scheme S the dependence of α_s^S on the scale μ is controlled by the renormalisation group through

$$\mu^2 \frac{d}{d\mu^2} \frac{\alpha_s^S(\mu^2)}{\pi} = \beta^S(\alpha_s^S) \sim - \sum_{i \geq 0} \beta_i^S \left(\frac{\alpha_s^S}{\pi} \right)^{i+2}, \quad (1.1)$$

where β^S is the beta function defined in that scheme. Its asymptotic expansion is known up to four loops in the $\overline{\text{MS}}$ scheme [2] and up to three loops in various MOM schemes [3]. The first two coefficients are renormalisation-scheme independent and can be looked up, e.g., in [4] and references therein. The number of physically admissible renormalisation schemes (RSs) is unlimited, and so is the number of running couplings. The $\overline{\text{MS}}$ scheme, with the underlying use of dimensional regularisation, is currently the most widely used RS in the analysis of high-energy experimental data. Such experiments are usually performed at different scales μ_i , but through Eq. (1.1) the different values of $\alpha_s^{\overline{\text{MS}}}(\mu_i)$ are related to each other.¹ In order to keep track of different initial parametrisations $(\mu_i, \alpha_s^{\overline{\text{MS}}}(\mu_i))$ a scale-invariant parameter $\Lambda^{\overline{\text{MS}}}$ is introduced. This can be done for any RS. Once the Λ parameter is known in one RS, a one-loop calculation is sufficient to obtain it in any other scheme (see, e.g., [7]).

Various nonperturbative studies in the past, in particular in lattice QCD, have provided estimates for $\alpha_s^{\overline{\text{MS}}}(M_Z)$ or $\Lambda^{\overline{\text{MS}}}$ for different numbers of flavour (see, e.g., [8–11]). There, different RSs, and thus different nonperturbative definitions of α_s , have been used and the results roughly agree with what has been found in experiment. Our objective here is to show that, in future, good results for $\alpha_s^{\overline{\text{MS}}}(M_Z)$ or $\Lambda^{\overline{\text{MS}}}$ may be expected using lattice QCD in Landau gauge.

The definition of the running coupling we employ here is a nonperturbative one that has been first presented in the context of introducing a solvable systematic truncation scheme for the Dyson-Schwinger equations of Euclidean QCD in Landau gauge [12]. This running coupling, which we call α_s^{MOM} in what follows, is defined in a MOM scheme and has its seeds in the ghost-gluon vertex in Landau gauge. To be specific, we use [12]

$$\alpha_s^{\text{MOM}}(q^2) := \alpha_s^{\text{MOM}}(\mu^2) Z(q^2, \mu^2) J^2(q^2, \mu^2) \quad (1.2)$$

which defines a nonperturbative running coupling that enters directly into the DSEs of QCD [13]. Z and J are the renormalised dressing functions of the gluon and ghost propagators,

$$D_{\mu\nu}^{ab}(q^2, \mu^2) = \delta^{ab} \left(\delta_{\mu\nu} - \frac{q_\mu q_\nu}{q^2} \right) \frac{Z(q^2, \mu^2)}{q^2} \quad \text{and} \quad G^{ab}(q^2, \mu^2) = -\delta^{ab} \frac{J(q^2, \mu^2)}{q^2}. \quad (1.3)$$

¹In the literature it is common practice to evolve data to $\alpha_s^{\overline{\text{MS}}}$ at the Z-Boson mass (see, e.g., [5, Fig.23] for a nice illustration.) A recent compilation of $\alpha_s^{\overline{\text{MS}}}(M_Z)$ values has been given at the ICHEP conference resulting in the world average $\alpha_s^{\overline{\text{MS}}}(M_Z) = 0.1175 \pm 0.0011$ [6].

In a lattice regularised theory, the corresponding bare dressing functions Z_L and J_L are related to Z and J , renormalised at some sufficiently large $q^2 = \mu^2$, by

$$Z(q^2, \mu^2) = Z_3^{-1}(\mu^2, a^2) Z_L(a^2, q^2) \quad \text{and} \quad J(q^2, \mu^2) = \tilde{Z}_3^{-1}(\mu^2, a^2) J_L(a^2, q^2) \quad (1.4)$$

where Z_3 and \tilde{Z}_3 are the respective renormalisation constants and a is the lattice spacing. When considering $1/a$ as our lattice UV cutoff, i.e., for $a \rightarrow 0$, then ²

$$\frac{g^2(a)}{4\pi} \frac{Z_3(\mu^2, a^2) \tilde{Z}_3^2(\mu^2, a^2)}{\tilde{Z}_1(\mu^2, a^2)} \xrightarrow{a \rightarrow 0} \alpha_s^{\text{MOM}}(\mu^2). \quad (1.5)$$

With discretisation errors of $O(a^2)$ we can thus write

$$\alpha_s^{\text{MOM}}(q^2) = \frac{g^2(a)}{4\pi} Z_L(q^2, a^2) J_L^2(q^2, a^2) + O(a^2), \quad (1.6)$$

where $g^2(a)$ is the bare coupling at the lattice cutoff scale $1/a$. It is this form of the running coupling which we will use below.

2. Details of the numerical simulation

The preliminary results described here were obtained on both zero and two-flavour $SU(3)$ gauge field configurations. The quenched configurations were thermalised using the standard Wilson gauge action at several values of $\beta \equiv 6/g^2(a)$. We applied update cycles each consisting of one heatbath and four micro-canonical over-relaxation steps. The unquenched gauge field configurations were provided to us by the QCDSF collaboration. They used the same gauge action but supplemented it by $N_f = 2$ clover-improved Wilson fermions at various values of the hopping-parameter κ . For details on the choice of β - and κ -values we refer to Tab. 1. All gauge configurations were fixed to Landau gauge with an iterative Fourier-accelerated gauge-fixing algorithm [18].³ For the stopping criterion we chose $\max_x \text{Tr} [(\nabla_\mu A_{x,\mu})(\nabla_\mu A_{x,\mu})^\dagger] < 10^{-13}$. The fields $A_{x,\mu} \equiv A_\mu(x + \hat{\mu}/2)$ are the lattice gluon fields given here in terms of gauge-fixed links $U_{x,\mu}$ by the mid-point definition

$$A_\mu(x + \hat{\mu}/2) := \frac{1}{2aig} (U_{x,\mu} - U_{x,\mu}^\dagger) - \frac{\mathbb{1}}{6aig} \text{Tr}(U_{x,\mu} - U_{x,\mu}^\dagger).$$

This is accurate to order $O(a^2)$. On each such gauge-fixed configuration the momentum-space gluon and ghost propagators were measured. On the lattice, these are defined as the Monte Carlo averages

$$D_{\mu\nu}^{ab}(k) = \left\langle \tilde{A}_\mu^a(k) \tilde{A}_\nu^b(-k) \right\rangle_U \quad \text{and} \quad G^{ab}(k) = \frac{1}{V} \left\langle \sum_{xy} (M^{-1})_{xy}^{ab} e^{ik \cdot (x-y)} \right\rangle_U$$

²Note that, in Landau gauge, as shown long ago [14], the ghost-gluon vertex is regular and finite to any order in perturbation theory. Its renormalisation constant can thus be set to $\tilde{Z}_1 = 1$. Numerical evidence that this is also valid nonperturbatively has been provided in various investigations (see, e.g., [15–17]).

³Note that for the range of momenta studied here the Gribov ambiguity is irrelevant as verified numerically in [19].

β	κ	latt.	a [fm]	#conf.	β	latt.	a [fm]	#conf.
5.25	0.13575	$24^3 \times 48$	0.084	60	–	–	–	–
5.29	0.13590	$24^3 \times 48$	0.080	55	6.20	32^4	0.063	30
5.40	0.13610	$24^3 \times 48$	0.070	62	6.40	32^4	0.048	50
5.40	0.13640	$32^3 \times 64$	0.068	57	6.60	32^4	0.037	60
5.40	0.13660	$32^3 \times 64$	0.068	30	6.80	32^4	0.029	46

Table 1: Number of $N_f = 2$ (left) and $N_f = 0$ (right) configurations used. To set the lattice spacings we use values for (r_0/a) as provided by QCDSF [9, 20] and assume $r_0 = 0.467$ fm.

where $\tilde{A}_\mu = \tilde{A}_\mu^a T^a$ are the Fourier-transformed gluon fields, M is the lattice Faddeev-Popov operator in Landau gauge, and $k \cdot x \equiv \sum_\mu 2\pi k_\mu x_\mu / L_\mu$. For a definition of M and details on its inversion we refer to [17, 19] and references therein. The corresponding bare dressing functions, Z_L and J_L , are then calculated by assuming a tensor structure for the lattice propagators as given in Eq. (1.3), but with the continuum momenta q_μ substituted by $p_\mu(k) = (2/a) \sin(\pi k_\mu / L_\mu)$ where the integers $k_\mu \in \{-L_\mu/2 + 1, \dots, L_\mu/2\}$.⁴ At tree level this tensor structure is exact for the Wilson gauge action and the Faddeev-Popov operator we use (applying periodic boundary conditions). Given the data for Z_L and J_L , we then estimate the coupling constant by the product

$$\alpha_L(p^2) = \frac{g^2(a)}{4\pi} Z_L(p^2, a^2) J_L^2(p^2, a^2) \quad (2.1)$$

where $g^2(a) = 6/\beta$. The corresponding error is obtained from a bootstrap analysis. Note that unlike other lattice investigations where data for Z and J are usually separately renormalised, no renormalisation is done here.

3. Preliminary results

In Fig. 1 (left) we show our present $N_f = 2$ data on α_L as a function of momentum. One sees that the data for different values of the input parameters β and κ form a reasonably smooth curve, indicating that discretisation effects are small for the input we employ. The only noticeable exceptions are the highest momentum values of each data set, where a slight deviation becomes evident with decreasing a . As expected, the quark-mass dependence is small.

Discretisation effects are more evident for our present quenched data, as shown in Fig. 1 (right). In particular for $\beta \leq 6.4$, which corresponds to even smaller lattice spacings than we use for $N_f = 2$, the data at larger momenta tends towards larger values as a decreases. Perhaps surprisingly, this effect is in the opposite direction than that observed in the unquenched data.

Since we use a tree-level improved definition of momentum (see above) the data at larger momenta is expected to be less affected by discretization errors than with the naive definition $a\tilde{p}_\mu = 2\pi k_\mu / L_\mu$. Nevertheless, if the data is fit to perturbative QCD, e.g., as described below, the momenta p_μ considered must satisfy $\Lambda \sim 250$ MeV $\ll |p_\mu| \ll \pi/a$. For the cylinder-cut data [21] used here, this translates into an upper bound of $p^2 = p_\mu p_\mu \ll 4\pi^2/a^2 \sim 300$ GeV² with the lattice spacings for $N_f = 2$ in Fig. 2. This leaves us a considerable range of momenta to work with.

⁴Of course, for both propagators the case $k \equiv (k_1, k_2, k_3, k_4) = 0$ has to be excluded.

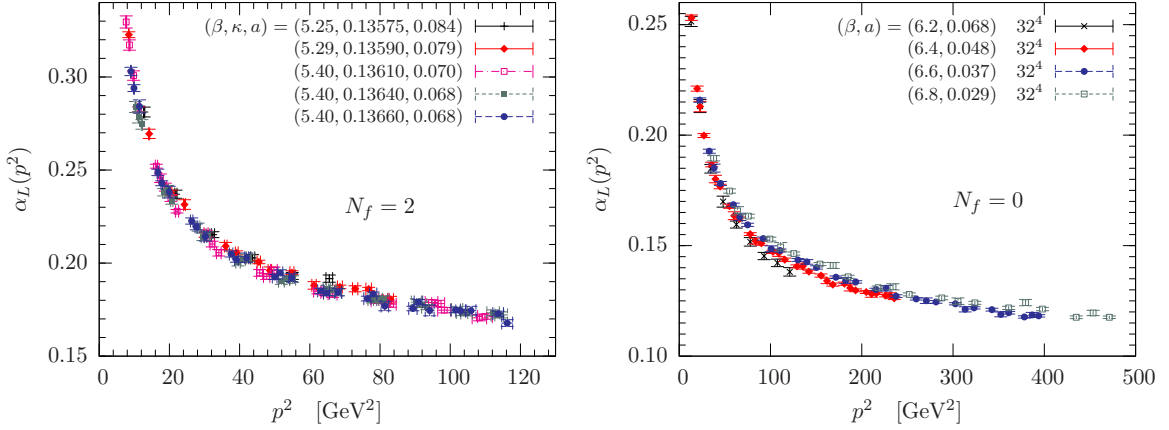


Figure 1: $N_f = 2$ (left) and $N_f = 0$ (right) data for $\alpha_L(p^2)$ at different β (and κ). We set $r_0 = 0.467$ fm to assign physical units to p^2 . Approximate values for the lattice spacing a are given in fm.

We observe, however, that for both the quenched and the unquenched data, strong discretisation effects appear at $a^2 p^2 \geq 14$ (not shown), where the data points (for fixed parameters) start bending downwards as $a^2 p^2$ is further increased. We therefore restrict the present analysis to momenta $a^2 p^2 < 14$ where no such effect occurs.

Given the data for different parameters, we consider, for each data set, a range of fitting windows within which the data is fit to a perturbative expansion of our running coupling. Since, from perturbative QCD, the running of α_s^{MOM} is known up to three loops for the ghost-gluon vertex [3], we could use the truncated α_s^{MOM} beta-function at 3-loop order from Ref. [3] to describe the running of our data. However, the coefficients c_1 and c_2 in the expansion of α_s^{MOM} in terms of $\alpha_s^{\overline{\text{MS}}}$, i.e.

$$\alpha_s^{\text{MOM}} = \alpha_s^{\overline{\text{MS}}} \left\{ 1 + c_1 \alpha_s^{\overline{\text{MS}}} + c_2 [\alpha_s^{\overline{\text{MS}}}]^2 + c_3 [\alpha_s^{\overline{\text{MS}}}]^3 + \dots \right\}, \quad (3.1)$$

which are known, as a function of N_f [3],⁵ are all positive and of $O(1)$ for the cases considered here, causing α_s^{MOM} to run more rapidly with scale than does $\alpha_s^{\overline{\text{MS}}}$. The result is that, as one lowers the scale, the truncated running at a given order becomes problematic at higher scales for the MOM coupling than it does for the $\overline{\text{MS}}$ coupling. In order to opt for the safest version of our analysis from the outset, we thus perform the running using the intermediate $\alpha_s^{\overline{\text{MS}}}$ running at four loops, with matching from α_s^{MOM} to $\alpha_s^{\overline{\text{MS}}}$ at the start, and then re-matching back to α_s^{MOM} at the end.

In practice, this means that for our fits we scan over a fine-grid interval of $\alpha_s^{\overline{\text{MS}}}$ values at an arbitrary reference scale μ , running each such value to all the momenta p^2 considered with the truncated 4-loop running⁶ relevant to N_f . At each p^2 the 4-loop value of $\alpha_s^{\overline{\text{MS}}}(p^2)$ is then related to the corresponding MOM value $\alpha_s^{\text{MOM}}(p^2)$ using the relation between the MOM and $\overline{\text{MS}}$ couplings given in Eq. (3.1). For this we use the known coefficients c_1 and c_2 and set $c_3 = c_4 = \dots = 0$, an approximation which appears to become reliable for sufficiently large p^2 in our data sets. A

⁵For the ghost-gluon vertex those coefficients are roughly $c_1(0) \approx 4.23/\pi$ and $c_2(0) \approx 36/\pi^2$ for the zero-flavour and $c_1(2) \approx 3.67/\pi$ and $c_2(2) \approx 26/\pi^2$ for the two-flavour case [3].

⁶To be specific, the running is performed using the exact analytic (implicit) solution of Eq. (1.1) corresponding to the four-loop truncated beta function.

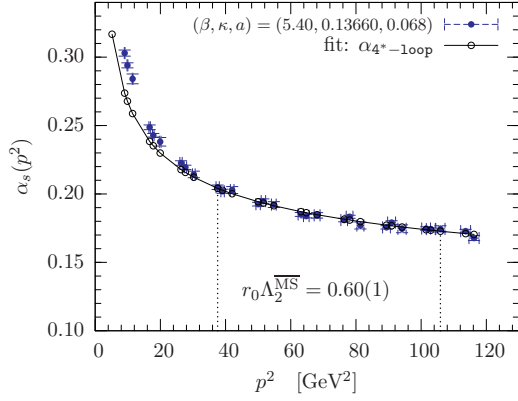


Figure 2: $N_f = 2$ data for $\alpha_L(p^2)$ at $\beta = 5.4$ and $\kappa = 0.1366$. The line represents the best fit to the data as described in the text. The fit window and the value of $r_0\Lambda^{\overline{\text{MS}}}$, as a result of that fit, are given too.

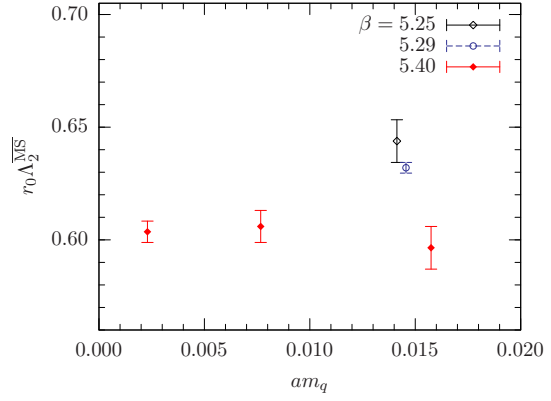


Figure 3: Fitted values for $r_0\Lambda_2^{\overline{\text{MS}}}$ as a function of bare mass am_q for different β . We use κ_c values from [9, 20] to set $am_q = (1/\kappa - 1/\kappa_c)/2$.

χ^2 -minimisation of the scaled deviations of $\alpha_s^{\text{MOM}}(p^2)$ from the $\alpha_L(p^2)$ data then determines the optimised $\alpha_s^{\overline{\text{MS}}}(\mu^2)$, from which the optimised $\Lambda^{\overline{\text{MS}}}$ value is obtained using the conventional definition given, e.g., in Ref. [22]. We perform such a fit separately on the data for each (β, κ, N_f) . An example of the resulting fit quality, together with the corresponding value for $r_0\Lambda^{\overline{\text{MS}}}$, is shown for the $(\beta, \kappa, N_f) = (5.4, 0.1366, 2)$ set in Fig. 2. Obviously, the data there is well described by the fit. The result shown there, $r_0\Lambda^{\overline{\text{MS}}} = 0.60(1)$, is already in the ballpark of what is expected based on the results of, e.g., Refs. [9, 11]. In Fig. 3 all our present (as-yet-preliminary) values of $r_0\Lambda^{\overline{\text{MS}}}$ for the $N_f = 2$ data sets are collected. Note that we have yet to fully investigate and quantify, and hence have not included in Fig. 3, uncertainties due to (i) truncated running, (ii) the impact of possible higher order, non-zero c_3, c_4, \dots terms in the relation between the $\overline{\text{MS}}$ and MOM couplings, and (iii) the statistical uncertainty in the fit associated with that in the data. In particular, this will then allow us to extrapolate our $r_0\Lambda^{\overline{\text{MS}}}$ values for the different parameters to the appropriate limits ($a \rightarrow 0, \kappa \rightarrow \kappa_c$) with realistic error estimates.

4. Conclusions

We have reported on first steps towards a determination of $\Lambda^{\overline{\text{MS}}}$ in terms of lattice MC simulations of gluodynamics within the Landau gauge. Our method is based on the ghost-gluon vertex which in this particular gauge provides a nonperturbative running coupling in a MOM scheme defined solely in terms of the gluon and ghost dressing functions. Both these dressing functions can be calculated in terms of lattice MC simulations with good accuracy.

Although our results are still preliminary, fits of our data to corresponding perturbative expressions of our running coupling result in values of $\Lambda_2^{\overline{\text{MS}}}$ in the range expected. This suggests that a full estimate of the QCD parameter Λ within this framework is worth pursuing. Different systematic effects still have to be investigated before final conclusions can be drawn. In addition to those already noted above, lattice discretisation errors, in particular for $N_f = 0$, need further study. In the light of the results shown in Fig. 2, however, the approach appears quite promising.

We thank the QCDSF collaboration for providing us their $N_f = 2$ gauge configurations. This research was supported by the Australian Research Council and by the Deutsche Forschungsgemeinschaft through the Research Group *Lattice Hadron Phenomenology* (FOR 465). K. M. acknowledges the ongoing support of the Natural Sciences and Engineering Council of Canada. Generous grants of time on the IBM pSeries 690 at HLRN (Germany) are acknowledged.

References

- [1] G. M. Prosperi, M. Raciti, and C. Simolo, *Prog. Part. Nucl. Phys.* **58** (2007) 387 [[hep-ph/0607209](#)].
- [2] T. van Ritbergen, J. A. M. Vermaseren, and S. A. Larin, *Phys. Lett.* **B400** (1997) 379 [[hep-ph/9701390](#)].
- [3] K. G. Chetyrkin and T. Seidensticker, *Phys. Lett.* **B495** (2000) 74 [[hep-ph/0008094](#)].
- [4] **Particle Data Group** Collaboration, W. M. Yao *et al.*, *J. Phys.* **G33** (2006) 1.
- [5] M. Davier, A. Hocker, and Z. Zhang, *Rev. Mod. Phys.* **78** (2006) 1043 [[hep-ph/0507078](#)].
- [6] S. Kluth, [hep-ex/0609020](#).
- [7] W. Celmaster and R. J. Gonsalves, *Phys. Rev.* **D20** (1979) 1420.
- [8] **HPQCD** Collaboration, Q. Mason *et al.*, *Phys. Rev. Lett.* **95** (2005) 052002 [[hep-lat/0503005](#)].
- [9] **QCDSF-UKQCD** Collaboration, M. Göckeler *et al.*, *Phys. Rev.* **D73** (2006) 014513 [[hep-ph/0502212](#)].
- [10] **ALPHA** Collaboration, S. Capitani, M. Lüscher, R. Sommer, and H. Wittig, *Nucl. Phys.* **B544** (1999) 669 [[hep-lat/9810063](#)].
- [11] **ALPHA** Collaboration, M. Della Morte *et al.*, *Nucl. Phys.* **B713** (2005) 378 [[hep-lat/0411025](#)].
- [12] L. von Smekal, R. Alkofer, and A. Hauck, *Phys. Rev. Lett.* **79** (1997) 3591 [[hep-ph/9705242](#)]; *Ann. Phys.* **267** (1998) 1 [[hep-ph/9707327](#)].
- [13] R. Alkofer and L. von Smekal, *Phys. Rept.* **353** (2001) 281 [[hep-ph/0007355](#)].
- [14] J. C. Taylor, *Nucl. Phys.* **B33** (1971) 436; W. J. Marciano and H. Pagels, *Phys. Rept.* **36** (1978) 137.
- [15] R. Alkofer, C. S. Fischer, and F. J. Llanes-Estrada, *Phys. Lett.* **B611** (2005) 279 [[hep-th/0412330](#)].
- [16] A. Cucchieri, T. Mendes, and A. Mihara, *JHEP* **12** (2004) 012 [[hep-lat/0408034](#)]; E.-M. Ilgenfritz, M. Müller-Preussker, A. Sternbeck, A. Schiller, and I. L. Bogolubsky, *Braz. J. Phys.* **37** (2007) 193 [[hep-lat/0609043](#)].
- [17] A. Sternbeck, PhD thesis, Humboldt-University Berlin, 2006, [hep-lat/0609016](#).
- [18] C. T. H. Davies *et al.*, *Phys. Rev.* **D37** (1988) 1581.
- [19] A. Sternbeck, E.-M. Ilgenfritz, M. Müller-Preussker, and A. Schiller, *Phys. Rev.* **D72** (2005) 014507 [[hep-lat/0506007](#)].
- [20] J. Zanotti, private communication.
- [21] **UKQCD** Collaboration, D. B. Leinweber, J. I. Skullerud, A. G. Williams, and C. Parrinello, *Phys. Rev.* **D60** (1999) 094507 [[hep-lat/9811027](#)].
- [22] K. G. Chetyrkin, B. A. Kniehl, and M. Steinhauser, *Phys. Rev. Lett.* **79** (1997) 2184 [[hep-ph/9706430](#)].